



HighShear Viscometry with a Rotational ParallelDisk Device

R. W. Connelly and J. Greener

Citation: *J. Rheol.* **29**, 209 (1985); doi: 10.1122/1.549828

View online: <http://dx.doi.org/10.1122/1.549828>

View Table of Contents: <http://www.journalofrheology.org/resource/1/JORHD2/v29/i2>

Published by the [The Society of Rheology](#)

Related Articles

Continuous lubricated squeezing flow: A novel technique for equibiaxial elongational viscosity measurements on polymer melts

J. Rheol. **54**, 1083 (2010)

The bucket rheometer for shear stress-shear rate measurement of industrial suspensions

J. Rheol. **51**, 821 (2007)

Authors' Response

J. Rheol. **49**, 1551 (2005)

Letter to the Editor: Comment on "Origin of concentric cylinder viscometry" [*J. Rheol.* **49**, 807–818 (2005)]. The relevance of the early days of viscosity, slip at the wall, and stability in concentric cylinder viscometry

J. Rheol. **49**, 1539 (2005)

On the gap error in parallel plate rheometry that arises from the presence of air when zeroing the gap

J. Rheol. **49**, 919 (2005)

Additional information on *J. Rheol.*

Journal Homepage: <http://www.journalofrheology.org/>

Journal Information: <http://www.journalofrheology.org/about>

Top downloads: http://www.journalofrheology.org/most_downloaded

Information for Authors: http://www.journalofrheology.org/author_information

ADVERTISEMENT



Anton Paar® USA
800-722-7556
info.us@anton-paar.com
www.anton-paar.com

High-Shear Viscometry with a Rotational Parallel-Disk Device

R. W. CONNELLY and J. GREENER, *Research Laboratories,
Eastman Kodak Company, Rochester, New York 14650*

Synopsis

A novel technique for measuring viscosity at high shear rates is described. The technique is an extension of a well-established method, parallel-disk viscometry, which has been limited traditionally to low shear rates ($<500 \text{ s}^{-1}$). Precision mounting of the disks a small distance apart (ca. $50 \text{ }\mu\text{m}$) allowed high shear rates ($>50,000 \text{ s}^{-1}$) to be attained without disrupting the torsional flow field, and thus *controlled* measurements of viscosity could be made at those shear rates. The presence of flow disturbances such as shear heating, surface fracture, and radial migration, common impediments in high-shear measurements, can be readily detected with a thixotropic loop program, and the effect of such disturbances can be separated from the actual rheological response of the fluid. Data are presented on some well-defined fluids, both Newtonian and shear-thinning, and the limitations of this technique are discussed.

INTRODUCTION

The rheological behavior of liquids at high shear rates is important technologically as it affects the hydrodynamics of many industrially important flows. Systems where high-shear rheology is critical include lubrication flows, high-speed coating processes, and certain polymer fabrication processes such as injection molding. Despite extensive research in this area,^{1,2} the behavior of liquids at high shear rates is fundamentally not well understood. It was contended, for example, that the viscosity of polymer solutions that exhibit shear-thinning effects should reach a second Newtonian plateau η_{∞} at high shear rates, which is expected to be somewhat higher than the pure-solvent viscosity.^{3,4} This plateau, however, has rarely been observed in steady-state shear experiments, and its precise nature has not been fully elucidated. In addition, many seemingly classical Newtonian liquids such as glycerin and ethylene glycol were claimed to exhibit non-

Newtonian effects at high shear rates, and their rheological response at those shear rates was purported to be significantly different from their low-shear behavior.^{1,5} The elastic response of viscoelastic liquids at high shear rates is also an unsolved problem.

A major obstacle in trying to resolve these questions has been the difficulty of making measurements at high shear rates under *well-controlled* conditions. Although it is usually not difficult to attain high shear rates in laboratory equipment, it is often difficult to discern the true rheological response of the liquid from its apparent behavior because of various disturbances that influence the hydrodynamics at high flow speeds. The most difficult problems facing the experimentalist are viscous heat generation and flow instabilities that arise at high shear rates.

Despite these difficulties, there have been a few fairly successful attempts to conduct measurements at high shear rates with capillary, Couette, and slit devices. Capillary viscometers, because of their relative simplicity, have been widely used for both low- and high-shear measurements.^{6,7} A major problem with such devices, however, is the difficulty of accounting for viscous heating and inertia effects, which are usually coupled. A complicating feature is the fact that viscous heating generally reduces viscosity, much like a rheological shear-thinning effect, and hence the two effects cannot be easily separated.⁸ The Couette device has been somewhat more popular in high-shear viscometric studies, mainly because it provides a closed system that can be better controlled and it requires small volumes of liquid. Most of the high-shear Couette viscometers used to date are based on designs by Barber⁹ and Merrill¹⁰ and have been used extensively by these researchers^{4,11} as well as by Porter and co-workers,¹²⁻¹⁴ who used a modified version of the Barber viscometer. The need to maintain small uniform gaps and good concentricity in the cylindrical system is a major difficulty with the Couette devices. Recently, Lodge¹⁵ developed a high-shear slit rheometer that can attain shear rates of $>10^6 \text{ s}^{-1}$. This rheometer, unlike the capillary and Couette devices, allows the measurement of normal stresses at high shear rates by the hole-pressure method. Rotational rheometers such as the cone-and-plate and the parallel-disk systems have not been used traditionally in high-shear rheometry, mainly because they are purported to develop flow

instabilities at fairly low shear rates ($<1000 \text{ s}^{-1}$).¹⁶ The onset of these instabilities, however, is not inherent to the level of shear, and the effective range of such devices can be extended by proper changes in the system. In fact, the critical shear rate for the onset of the various flow instabilities in the cone-and-plate and the parallel-disk systems can be significantly increased by decreasing the gap separating the two members of the rheometer. This idea was exploited by Walters and co-workers^{17,18} in the development of the torsional balance rheometer, which was designed specifically for measuring normal stresses at high shear rates. In this study, we use a similar idea to extend the effective range of a conventional parallel-disk system.

THE PARALLEL-DISK SYSTEM

The parallel-disk system (PDS), sketched schematically in Figure 1, is a conventional rheometer used routinely for measuring rheological properties of liquids and rubbers.¹⁶ The PDS is operated by placing a small amount of liquid between two parallel plates, one of which is rotated at a constant angular speed Ω while the other is stationary. The torsional flow field generated in the gap between the plates is inhomogeneous, with the shear rate varying radially. The torque J required to maintain steady rotation at the specified speed is measured and converted to shear stress by use of the relationship¹⁹

$$\tau_R = \frac{J}{2\pi R^3} \left(3 + \frac{d \ln (J/2\pi R^3)}{d \ln \dot{\gamma}_R} \right), \quad (1)$$

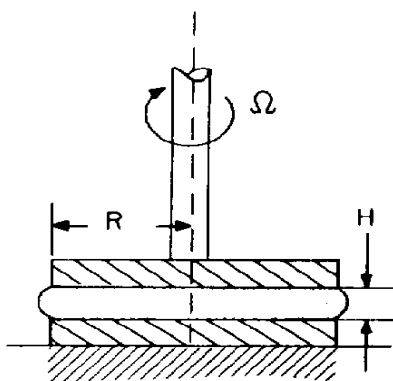


Fig. 1. The parallel-disk system.

where $\dot{\gamma}_R$, the nominal shear rate, is given by

$$\dot{\gamma}_R = \Omega R/H. \quad (2)$$

The subscript R indicates that the quantity is evaluated at the rim ($r = R$) of the device. Clearly, $\dot{\gamma}_R$ can be increased by increasing the speed of rotation and/or decreasing the gap separating the plates. The derivative on the right-hand side of Eq. (1) is the "non-Newtonian correction" to the stress, and, much like the Weissenberg–Mooney–Rabinowitsch correction in capillary flow,¹⁹ it originates from the inhomogeneity of the shear field in torsional flows. For Newtonian liquids this term is unity, but for shear-thinning liquids it is <1 . Equation (1) is valid in the limit of negligible inertia forces and isothermal conditions. Also, insofar as the nominal shear rate is evaluated at the rim of the device, the surface tension of the liquid and the general shape of the interface at $r = R$ are expected to have considerable effect on the apparent torque. Indeed, the two main failures in rotational rheometers, radial migration and surface fracture,¹⁶ are associated in some way with the dynamics of the interface at the rim.

Radial migration is an inertial instability caused by large centrifugal forces. When these forces are greater than the surface tension force that confines the liquid to the gap between the plates, the liquid will migrate radially and ultimately will be thrown out of the gap. Thus, for radial migration to occur, the centrifugal stress must exceed the surface-tension stress²⁰

$$\frac{3}{20} \rho \Omega^2 R^2 > \sigma/H, \quad (3a)$$

where ρ is the density and σ is the surface tension. Equation (3a) can be cast in terms of a critical shear rate,

$$\dot{\gamma}_c = \frac{1}{H} \sqrt{\frac{20\sigma}{3\rho H}}. \quad (3b)$$

This result defines the shear rate for the onset of radial migration and suggests that this instability can be eliminated by operating at small gaps and low speeds. Note that Eq. (3a) is valid strictly for inelastic liquids. Viscoelastic liquids will develop radial "hoop" stresses in torsional and cone-and-plate flows that would tend to stabilize the system with regard to the radial migration problem. However, the stability of viscoelastic liquids will usually be dic-

tated by a different sort of failure, which in most cases is far more serious. Above some critical speed the interface at the rim "fractures", i.e., the surface caves in toward the axis, and the system departs from its idealized shape.^{16,20-22} Fracture is usually accompanied by a large drop in torque and normal force and a pseudo-thixotropic (hysteresis) response. Hutton²² explained this effect in terms of a critical elastic strain energy and showed that fracture occurs when

$$N_1 > k\sigma/H, \quad (4)$$

where N_1 is the first normal stress difference and k is a constant parameter. More recently Tanner and Keentok²⁰ have shown, based on fracture mechanics arguments, that the condition for fracture is

$$|N_2| > 2\sigma/3a, \quad (5)$$

where N_2 is the second normal stress difference and a is the size of the fracture [normally, $a = O(H)$]. As pointed out by Tanner and Keentok, the above result is not in variance with Eq. (4) because, in general, $N_1 \propto N_2$. Equation (5) suggests that fracture is caused by the radial hoop stress, which tends to force the liquid toward the axis of the apparatus (opposite of radial migration). For this to happen, the radial stress must overcome the surface tension force, which tends to minimize the surface energy at the rim. Thus, depending on the rheological character of the liquid, the stability of the torsional flow system may be dictated either by the radial migration effect [Eq. (3a)] or by the surface fracture problem [Eqs. (4) and (5)]. In any case, it is evident that the effective range of the PDS viscometer can be increased if the gap between the plates is reduced.

EXPERIMENTAL

The high-shear-rate experiments were run with a conventional rotational rheometer operated in the parallel-disk mode. This rheometer is a subsystem of the Rheometrics System Four (the "Steady Head"). This system was selected because it offers a wide range of operational shear rates and it provides the precision and rigidity essential in high-shear measurements. Also, this system uses a torque transducer (2000 g cm) that covers the anticipated

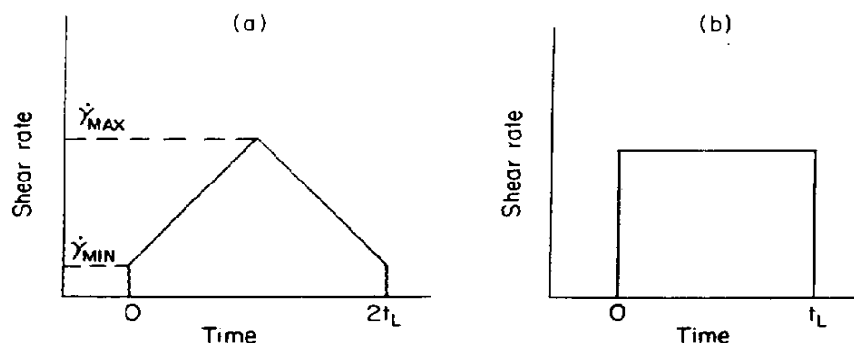


Fig. 2. Shear-rate programs: (a) thixotropic loop, (b) double-step shear-rate jump.

range of stress, and it provides a fast response and the necessary sensitivity.

To attain high shear rates, we used relatively large plates ($R = 2.5$ cm), and the gap between the plates was kept very small, ca. $50\text{ }\mu\text{m}$. The highest shear-rate for this setup is 10^5 s^{-1} . The high-shear measurements were run with two shear-rate programs (Fig. 2). The first is a conventional thixotropic loop (T-loop) in which the shear rate is ramped at a given rate from some starting value $\dot{\gamma}_{\min}$ up to $\dot{\gamma}_{\max}$, and then it is ramped down at the same rate back to the starting value. The second program, a double-step shear-rate jump, was used only to assess the effect of shear heating.

The T-loop was particularly useful in detecting the presence of disturbances such as radial migration, surface fracture, and viscous heating, which are usually manifested by a pseudo-thixotropic response. Generally, the loop time t_L was selected to be as short as possible to minimize potential shear-heating effects. (This point is discussed more fully in the next section.) For viscoelastic fluids, a "fast" loop may not be desirable because it may give rise to overshoot and other transient effects, which are also a disturbance in the sense of Eq. (1). However, these effects also would be manifested by a pseudo-thixotropic response and could be identified easily with a T-loop program.

Table I lists the liquids tested. The first two, S-20 and S-200, are standard silicone oils known to be Newtonian over a wide range of shear rates. These liquids were used for calibrating the viscometer and for assessing the effect of shear heating in the high-shear experiments. The other liquids are aqueous polymer

TABLE I
Test Liquids

Liquid	Source	C (wt %)	\bar{M}_w
S-20	Cannon Instruments	—	—
S-200	Cannon Instruments	—	—
PVP K-15	GAF	39.2	6900
PVP K-30	GAF	27.6	27,200
PVP K-60	GAF	14.4	136,000
PVP K-90	GAF	6.1	680,000
Separan MG-500	Dow	0.15	$>10^6$

solutions with concentrations as specified. The PVP's are a homologous series of polyvinylpyrrolidones with molecular weights as noted in Table I. For the compositions used, the PVP solutions were generally mildly shear thinning. The Separan MG-500, on the other hand, is a high-molecular-weight ($>10^6$) polyacrylamide known to form highly elastic and strongly shear-thinning solutions. A conventional Couette viscometer (Epprecht Rheomat 15) and the Fluids system of the Rheometrics System Four were used for obtaining low-shear rheological data on the test liquids.

Because of the unusually small gaps used in the high-shear runs, the alignment of the system, the flatness, concentricity, and smoothness of the plates, and the cleanness of the test liquid were all crucial to the success of this experiment. Although the test system is precision machined, tolerance errors of $\pm 8 \mu\text{m}$ for parallelism, $\pm 10 \mu\text{m}$ for concentricity, and $\pm 3 \mu\text{m}$ for flatness were sufficient to introduce significant error in the measurement when the smallest gaps were used. To minimize the effect of these geometric imperfections, we calibrated the system with the standard oils. Measurements were made at several gap settings ranging from 0.05 to 0.6 mm, and the results were compared with low-shear data obtained with the Couette viscometer.

Generally, the high-shear runs yielded lower viscosities at the low gaps regardless of the oil used. As the gap increased, the apparent viscosity approached the "true" Newtonian viscosity of the oil. This suggested that the effective gap must be somewhat higher than the nominal gap such that

$$H_{\text{eff}} = H + \xi. \quad (6)$$

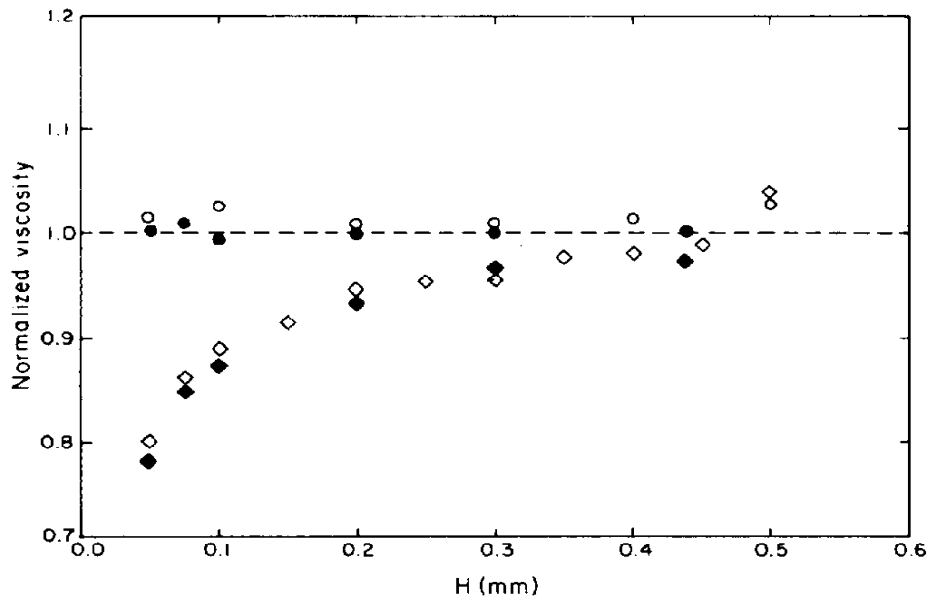


Fig. 3. Normalized viscosity versus gap separation: (\circ , \bullet) corrected and (\diamond , \blacklozenge) uncorrected data (S-200, open symbols; S-20, solid symbols).

Here ξ is a correction term that practically accounts for deviations from parallelism, concentricity, and flatness. Because the viscosity of the standard oil is independent of the gap setting, one may write in general [see Eq. (1)]

$$\frac{J_i(H_i + \xi)}{\Omega_i} = \frac{J_j(H_j + \xi)}{\Omega_j}, \quad (7)$$

where the subscripts i, j correspond to a pair of runs with different gap separations and angular speeds. Equation (7) was solved for ξ with data for both oils and several gap settings. A value of 14.4 μm was obtained from many data pairs with a small standard deviation. The corrected and uncorrected viscosities for both oils are plotted in Figure 3 versus gap separation. The viscosity in this plot is normalized with a value obtained from the low-shear measurements. Expectedly, the "geometric" error is independent of viscosity but depends on the gap separation, being largest for the smallest gaps. Figure 3 also shows that the correction of Eq. (6) is effective in overriding some of the geometric imperfections of the system.

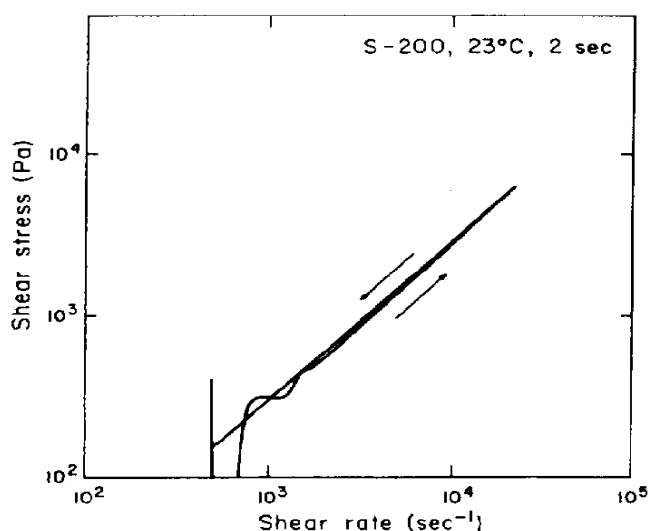


Fig. 4. Shear stress/shear rate loop for S-200: $t_L = 2$ s, 23°C .

RESULTS AND DISCUSSION

A T-loop program (see Fig. 2) was used in all the high-shear runs to assess the presence of disturbances in the torsional flow experiments. Figure 4 shows a typical stress-strain rate loop for the S-200 oil with $\dot{\gamma}_{\min} = 500 \text{ s}^{-1}$, $\dot{\gamma}_{\max} = 25,000 \text{ s}^{-1}$, and $t_L = 2$ s. The absence of hysteresis in the loop suggests that this run was free of disturbances and that the corresponding data represent the "true" rheological response of the liquid. The oscillations at the start of the loop (see also Fig. 9) are an artifact that represents the attempt of the servo unit to lock onto the specified shear rate. Data for the standard oils, covering nearly four decades in shear rate, are shown in Figure 5. Both oils are Newtonian over the experimental shear-rate range, and a good match is obtained between the low- and high-shear data.

Flow curves for the PVP series are shown in Figure 6. Here, only the low-MW polymer solutions, K-15 and K-30, are Newtonian up to the highest shear rate ($50,000 \text{ s}^{-1}$). The high-MW members of this series, K-60 and K-90, exhibit a distinct shear-thinning character, which is more pronounced the higher the molecular weight. This result is consistent with previous work.²³ As before, a good match between the high- and low-shear data is found. In all the data presented so far, no disturbances were de-

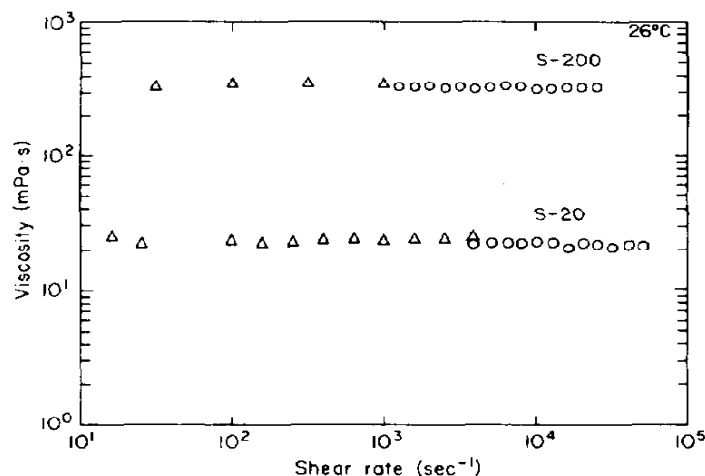


Fig. 5. Viscosity versus shear rate for the standard oils, 26°C.

tected up to the highest shear rate. Similar runs with the Separan solution were less successful.

Figure 7 shows T-loops for two Separan solutions with a loop time of 2 s. As in most attempts with the Separan liquids, these solutions displayed large overshoot and pronounced hysteresis, with the viscosity generally increasing with time. When the results of this run were compared with the low-shear data, a large discrepancy was found, especially at the low shear rates close to

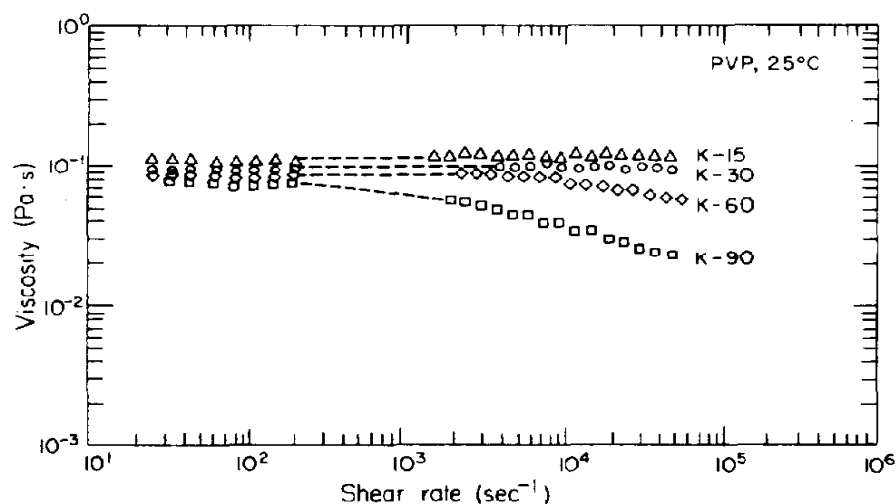


Fig. 6. Viscosity versus shear rate for the PVP solutions, 25°C: (Δ) K-15, (\circ) K-30, (\diamond) K-60, (\square) K-90.

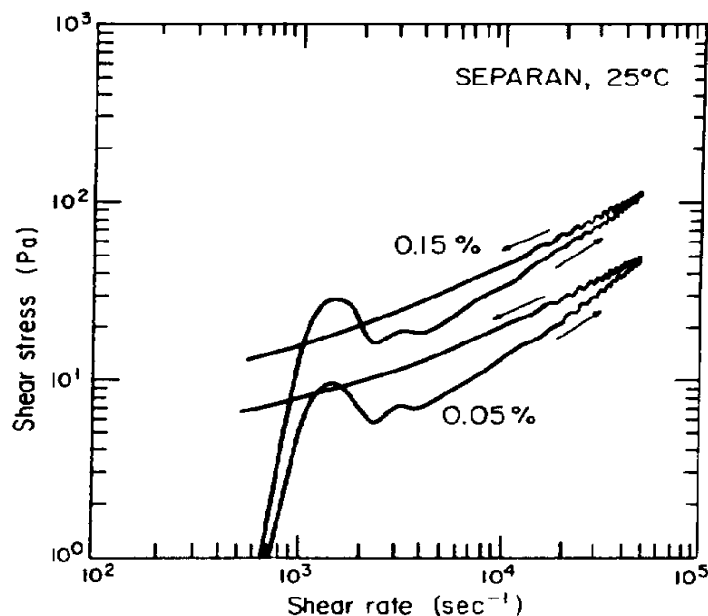


Fig. 7. Thixotropic loops for the Separan solutions, 25°C.

the start of the loop. This may be attributed to surface fracture, which apparently develops at the beginning of the run because of the large stress overshoots at start-up. The overshoot, which clearly can be identified in the traces in Figure 7, is a manifestation of the elasticity of the Separan solutions.

To overcome this problem, we tried to "smooth" the start-up phase by adding a "slow" step at the start of the T-loop ($0 \rightarrow 500 \text{ s}^{-1}$, 10 s) and then commencing with the regular T-loop program. This step helped eliminate the sharp stress overshoots at start-up and removed the hysteresis. This result suggests that the overshoot effect was indeed associated with the hysteresis in the dynamic response. A similar phenomenon was observed elsewhere and it was given a similar interpretation (cf. Ref. 16, p. 73). When the "smooth" trace was used to construct the viscosity curve, a good match with the low-shear data was found. This is shown in Figure 8, where the viscosity function of the 0.15% Separan solution is plotted. The low-shear data in this figure were obtained with a conventional Couette device (Epprecht Rheomat 15).

To outline the limitations of the high-shear PDS viscometer, we give below a brief and critical assessment of the main flow disturbances in this system.

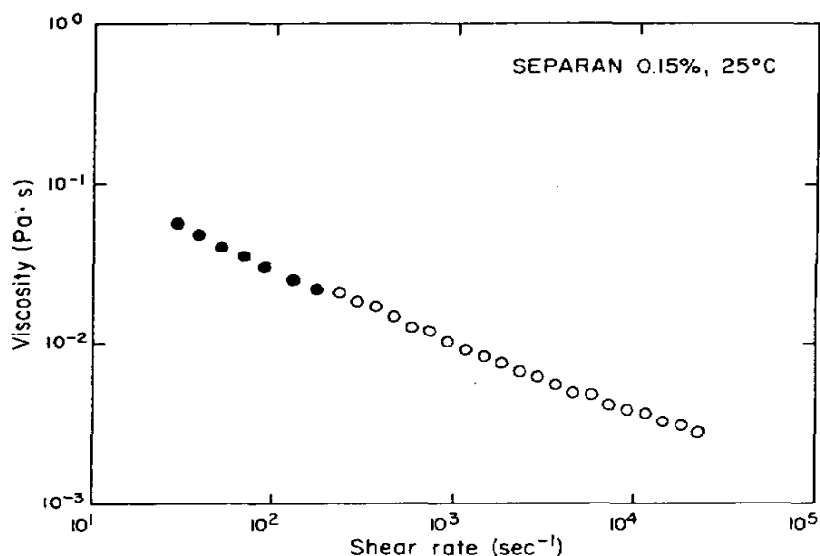


Fig. 8. Viscosity versus shear rate for the 0.15% Separan solution, 25°C.

Viscous Heating

Because it manifests itself like a rheological shear-thinning effect, viscous heating is one of the disturbances most difficult to account for in high-shear viscometry. As was noted, this disturbance can be readily detected with a T-loop program. This is illustrated in Figure 9, where several stress-strain rate traces are presented corresponding to different loop times. In all cases $\dot{\gamma}_{\min} = 1000 \text{ s}^{-1}$, $\dot{\gamma}_{\max} = 35,000 \text{ s}^{-1}$, and the liquid is S-200. An increase in t_L enhances the hysteresis in the response curve. This effect is apparently caused by shear heating, and it implies that by operating at small t_L 's (less than 2 s for most cases in this study) it is possible to practically eliminate the problem. Essentially, in a fast run, the temperature does not rise enough to affect the properties and apparent response of the liquid. Obviously, the critical value of t_L will depend principally on the viscosity of the liquid and on $\dot{\gamma}_{\max}$.

To examine the effect of shear heating more closely, we ran several experiments with the standard oils, using the double-step jump program [Fig. 2(b)]. The level of shear rate varied, but the loop time for these runs was 40 s. Figure 10, representing stress histories for all the runs, clearly shows that shear heating can have a strong effect on the apparent response. Generally, from

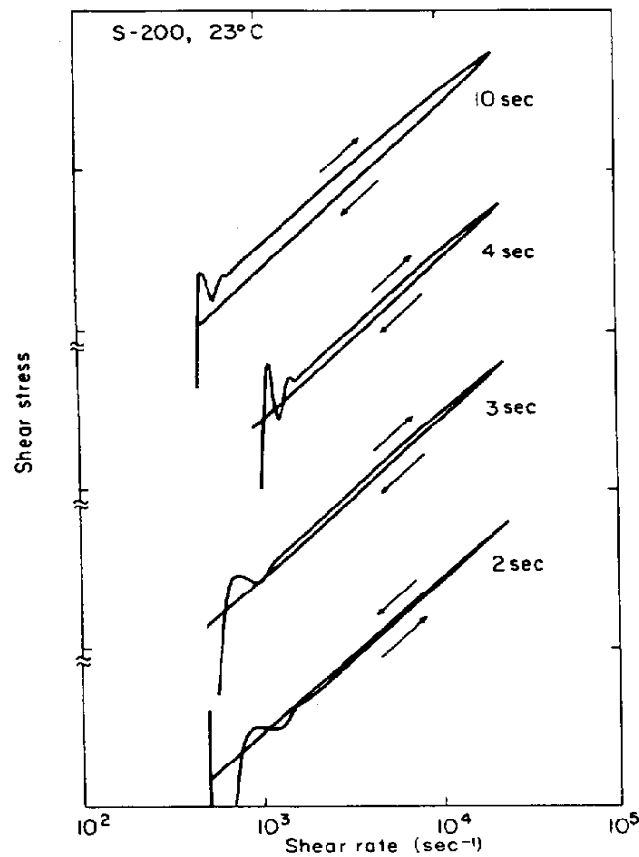


Fig. 9. Shear stress/shear rate loops for different loop times: the liquid is S-200, 23°C.

knowledge of the temperature dependence of viscosity, one can estimate the temperature rise due to viscous heating, using the data in Figure 10. For an Arrhenius-activated flow, the viscosity is given by

$$\mu = A \exp (b/T), \quad (8)$$

and the temperature rise corresponding to the change in stress is

$$\Delta T \cong -\frac{1}{b} \frac{\Delta \tau}{\bar{\tau}_0} \bar{T}^2, \quad (9)$$

where \bar{T} is the average value of temperature for the duration of the run and $\bar{\tau}_0$ is the initial value of the shear stress. The extent of

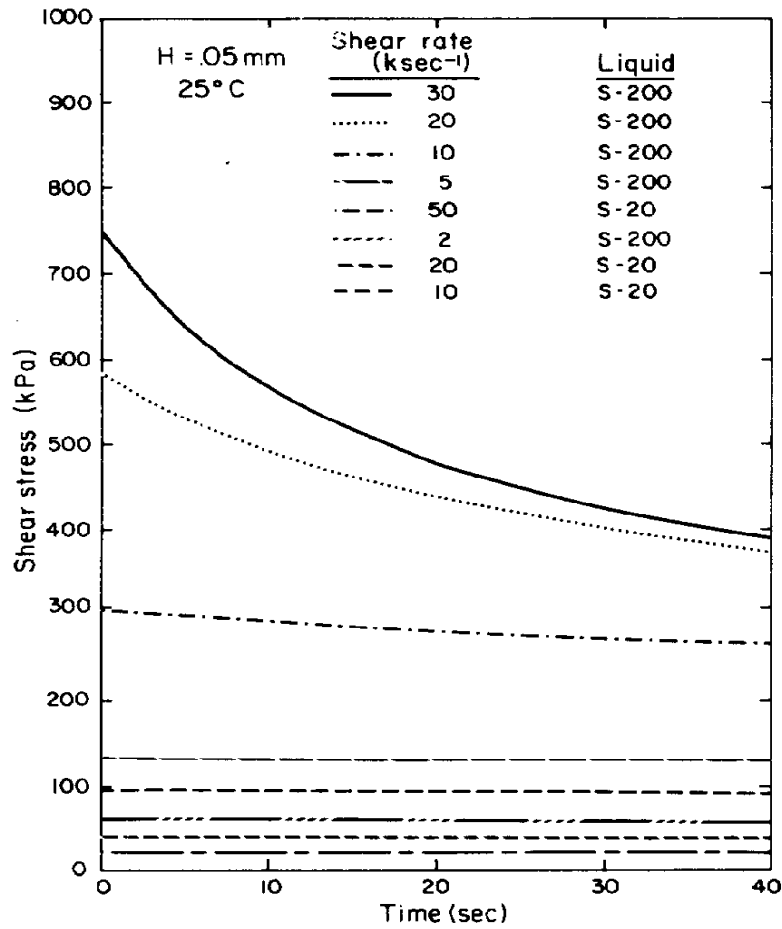


Fig. 10. Shear stress versus time for the standard oils at different shear rates. $H = 0.5$ mm, 25°C .

temperature rise is expected to depend on a characteristic shear-heating parameter, which, for this case, is best represented by the Nahmé-Griffith number,^{24,25}

$$N_{\text{NG}} = \frac{\mu \Omega^2 R^2}{\kappa \Delta T_{\text{rheol}}}, \quad (10)$$

where κ is the thermal conductivity and ΔT_{rheol} represents the temperature dependence of viscosity,

$$\Delta T_{\text{rheol}} = \frac{-\mu}{(d\mu/dT)} = \frac{\bar{T}^2}{b}. \quad (11)$$

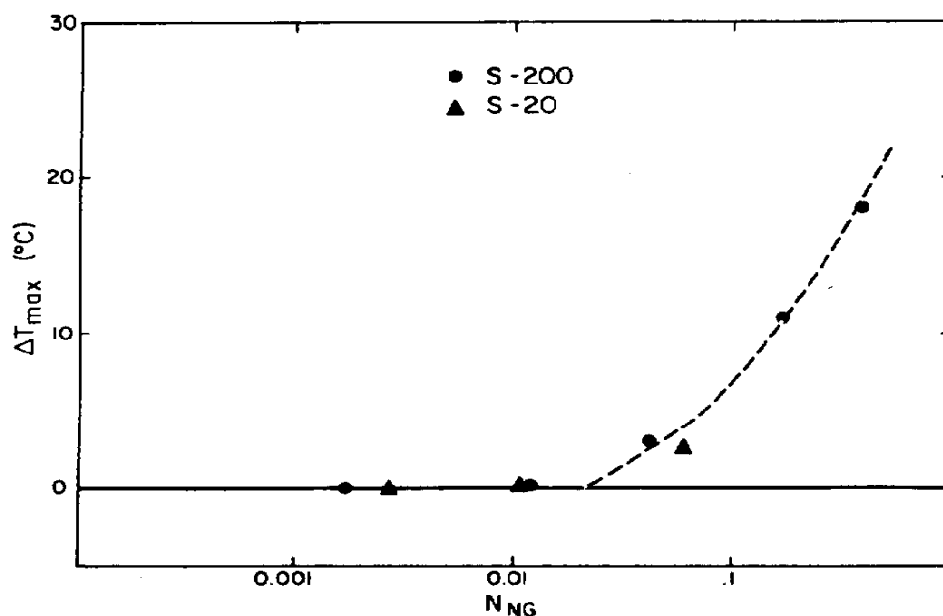


Fig. 11. The maximum temperature rise versus the Nahmé-Griffith number: (●) S-200, (▲) S-20.

Using Eqs. (9) and (10), we correlated the data in Figure 10 in terms of the maximum temperature rise (ΔT at 40 s) versus the corresponding value of N_{NG} (Fig. 11). The extent of shear heating, as represented by ΔT_{max} , correlates well with N_{NG} , and there appears to be a critical value of N_{NG} (ca. 0.02) below which shear-heating effects are expected to be negligible. This criterion is generally conservative, because the values of ΔT_{max} in Figure 11 correspond to relatively long residence times.

Radial Migration

The criterion for radial migration, Eq. (3), can be formulated in terms of a dimensionless number, $N_{RM} = \sigma/\rho H \Omega^2 R^2$. Based on Eq. (3), radial migration will occur when $N_{RM} < 0.15$.

Thus, the group σ/ρ is generally stabilizing, whereas $H \Omega^2 R^2$ is destabilizing. For the liquids in this study, σ/ρ varies in the range 30–70 cm³s⁻². If we take $H = 0.005$ cm, the critical speed $(\Omega R)_c$ will vary in the range 75–120 cm/s, and the critical shear rate will fall within 80,000–115,000 s⁻¹. For a gap larger by a factor of 10, the critical shear rate will decrease by a factor of 32, thus

limiting the apparatus to fairly low shear rates. Tanner and Keentok²⁰ have noted that meaningful measurements can be made at, or even above, the critical shear rate, if shear is applied for a very short time so that the instability does not have time to establish itself. This can be accomplished in our system by "fast" T-loops. In general, however, the above results suggest that radial migration should not be a serious problem in the PDS viscometer under the conditions of this study.

Surface Fracture

Surface fracture is usually a more serious problem than radial migration, especially for highly elastic liquids. This problem is also more difficult to assess because reliable information on the elastic stresses N_1 [Eq. (4)] or N_2 [Eq. (5)] at very high shear rates is not readily available. If we take some typical values, $\sigma = 50$ dyn/cm, $a = 0.33H$, and $H = 0.005$ cm, then, using the Tanner-Keentok criterion [Eq. (5)], we get $N_{2c} \cong -2000$ Pa. Furthermore, assuming that $N_{2c} \cong -0.1 N_1$,¹⁹ we find that $N_{1c} \cong 20,000$ Pa. This is a fairly high value for typical viscoelastic liquids, and it can be attained only if the liquid is very elastic and/or the shear rate is very high.

Figure 12 presents N_1 versus shear-rate data for the 0.15% Separan solution as measured with a conventional cone-and-plate device (the Fluids system of the Rheometrics System IV). If the N_1 function is simply extrapolated, the critical shear rate for the onset of surface fracture is ca. 10^6 s^{-1} , which is well beyond the operational range of the instrument. This excludes the presence of stress overshoots at the start-up of the T-loop, which in itself may be a strongly destabilizing factor, as is evident from the results in Figure 7. Finally, because of the small gaps in the high-shear setup, direct detection of surface fracture is difficult, if not impossible. This instability can only be inferred, with some uncertainty, from the T-loop response of the liquid.

SUMMARY

A conventional parallel-disk viscometer can be used to measure viscosity at high shear rates ($>10^4 \text{ s}^{-1}$) if the gap between

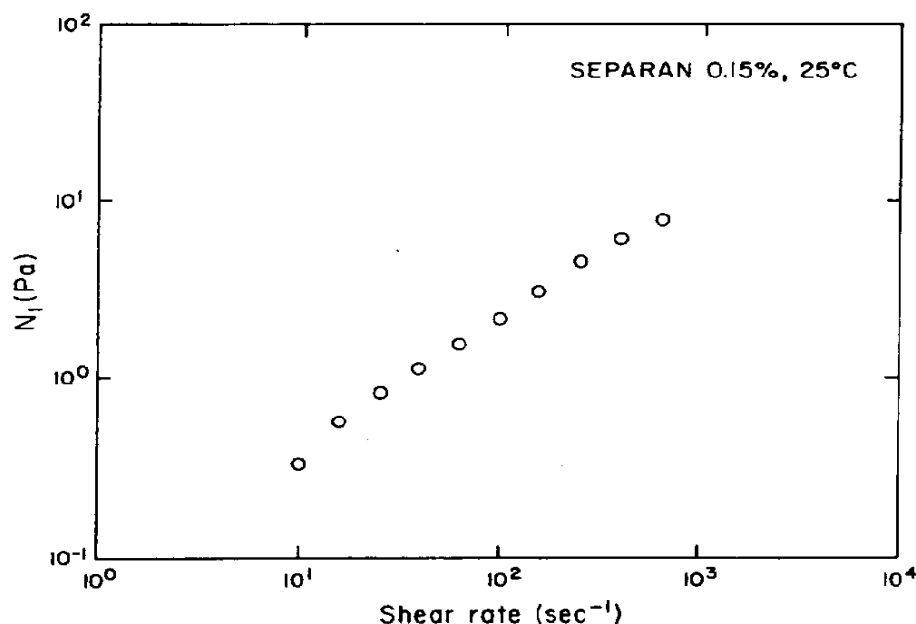


Fig. 12. First normal stress difference versus shear rate for the 0.15% Separan solution, 25°C.

the plates can be kept very small, <0.1 mm. With small gaps, not only is the nominal shear rate increased, but some of the flow instabilities that are common in torsional flows can be largely eliminated. This generally will not apply to highly elastic liquids, such as polyacrylamide solutions, which are likely to develop flow instabilities at relatively low shear rates, even for very small gaps. Of particular concern here are stress overshoots, which may severely disrupt the torsional flow field and thereby introduce large errors into the viscosity measurements. This problem can be partly alleviated by "smoothing out" the start-up phase of the T-loop, as is demonstrated by the results of Figure 8. In general, if the run is conducted with a thixotropic loop program, flow disturbances such as viscous heating and inertia can be readily detected, and the quality of the data can be instantly and critically assessed.

We thank Ms. Bev Contestable for her help in obtaining the low-shear viscosity data. The molecular weights of the PVPs were supplied by Dr. M. Sterman.

References

1. A. Ram, in *Rheometry*, Vol. 4, F. Eirich, Ed., Academic, New York, 1967.
2. J. R. Van Wazer, J. W. Lyons, K. Y. Kim, and R. E. Colwell, *Viscosity and Flow Measurements*, Wiley, New York, 1963.
3. E. W. Merrill, *J. Polym. Sci.*, **38**, 539 (1959).
4. E. W. Merrill, H. S. Mickley, A. Ram, and W. H. Stockmayer, *J. Polym. Sci., Part A*, **1**, 1201 (1963).
5. E. W. Merrill, in *Modern Chemical Engineering*, A. Acrivos, Ed., Reinhold, New York, 1963.
6. J. G. Brodnyan and E. L. Kelley, *Trans. Soc. Rheol.*, **5**, 205 (1961).
7. B. J. Meister and R. D. Biggs, *AIChE J.*, **15**, 643 (1969).
8. A. Dyson, *Philos. Trans. R. Soc. London*, **258**, 66 (1965).
9. E. M. Barber, J. R. Muenger, and F. J. Villforth, *Anal. Chem.*, **27**, 425 (1955).
10. E. W. Merrill, *ISA J.*, **3**, 173 (1956).
11. E. W. Merrill, H. S. Mickley, A. Ram, and G. Perkinson, *Trans. Soc. Rheol.*, **5**, 237 (1961).
12. R. S. Porter and J. F. Johnson, *Trans. Soc. Rheol.*, **9**, 45 (1965).
13. L. A. Manrique, Jr., and R. S. Porter, *Rheol. Acta*, **14**, 926 (1975).
14. W.-M. Kulicke and R. S. Porter, *J. Polym. Sci. Polym. Phys. Ed.*, **19**, 1173 (1981).
15. A. S. Lodge, *IUPAC 28th Macromolecular Symp.*, University of Massachusetts, Amherst, MA, 1982.
16. K. Walters, *Rheometry*, Wiley, New York, 1975.
17. D. M. Binding and K. Walters, *J. Non-Newt. Fluid. Mech.*, **1**, 277 (1976).
18. K. Walters, *Proc. VII Int. Congr. Rheology*, J. Kubat, Ed., Gothenburg, Sweden, 1976.
19. R. B. Bird, R. A. Armstrong, and O. Hassager, *Dynamics of Polymeric Liquids*, Vol. 1, Wiley, New York, 1977.
20. R. C. Tanner and M. Keentok, *J. Rheol.*, **27**, 47 (1983).
21. J. F. Hutton, *Proc. R. Soc. London, Ser. A*, **287**, 222 (1965).
22. J. F. Hutton, *Rheol. Acta*, **8**, 54 (1969).
23. W. W. Graessley, in *Advances in Polymer Science*, Vol. 16, Springer-Verlag, New York, 1974.
24. H. H. Winter, *Adv. Heat Transfer*, **13**, 205 (1977).
25. J. R. A. Pearson, *Polym. Eng. Sci.*, **18**, 222 (1978).

Received December 3, 1983

Accepted April 16, 1984